

This article was downloaded by:

On: 25 January 2011

Access details: *Access Details: Free Access*

Publisher *Taylor & Francis*

Informa Ltd Registered in England and Wales Registered Number: 1072954 Registered office: Mortimer House, 37-41 Mortimer Street, London W1T 3JH, UK



## Separation Science and Technology

Publication details, including instructions for authors and subscription information:

<http://www.informaworld.com/smpp/title~content=t713708471>

### Two Different Configurations of Flow Field-Flow Fractionation for Size Analysis of Colloids

Jocelyne Granger<sup>a</sup>; John Dodds<sup>a</sup>

<sup>a</sup> LABORATOIRE DES SCIENCES DU GÉNIE CHIMIQUE CNRS-ENSC, NANCY, FRANCE

**To cite this Article** Granger, Jocelyne and Dodds, John(1992) 'Two Different Configurations of Flow Field-Flow Fractionation for Size Analysis of Colloids', *Separation Science and Technology*, 27: 13, 1691 — 1709

**To link to this Article:** DOI: 10.1080/01496399208019441

URL: <http://dx.doi.org/10.1080/01496399208019441>

## PLEASE SCROLL DOWN FOR ARTICLE

Full terms and conditions of use: <http://www.informaworld.com/terms-and-conditions-of-access.pdf>

This article may be used for research, teaching and private study purposes. Any substantial or systematic reproduction, re-distribution, re-selling, loan or sub-licensing, systematic supply or distribution in any form to anyone is expressly forbidden.

The publisher does not give any warranty express or implied or make any representation that the contents will be complete or accurate or up to date. The accuracy of any instructions, formulae and drug doses should be independently verified with primary sources. The publisher shall not be liable for any loss, actions, claims, proceedings, demand or costs or damages whatsoever or howsoever caused arising directly or indirectly in connection with or arising out of the use of this material.

## Two Different Configurations of Flow Field-Flow Fractionation for Size Analysis of Colloids

JOCELYNE GRANGER and JOHN DODDS

LABORATOIRE DES SCIENCES DU GÉNIE CHIMIQUE

CNRS-ENSC

1 RUE GRANDVILLE, B.P. 451, 54001 NANCY, FRANCE

### Abstract

Flow field-flow fractionation (F.FFF) is a technique for measuring the size of species in the colloidal range (1 nm to 1  $\mu\text{m}$ ) which makes the use of the formation of a molecular or colloidal polarization layer at the surface of a filtering membrane. The species to be analyzed are introduced into a flow of liquid passing through a channel with porous walls (of pore size less than that of the colloids to be analyzed) which allow a certain controlled flow to pass through. The remaining fraction of the flow passes through the system, carrying the colloids to a nonspecific detector. The transit time of the colloids through the channel is found to be a function of their size and the permeation rate through the porous membrane. This chromatographic system can be calibrated by using known colloids, such as standard latex particles or fractionated polymer samples, and then used to determine the size of unknown colloids. Here we present results obtained in two different systems, an asymmetric module with a rectangular channel having a single flat membrane and a module based on a hollow ultrafiltration fiber with a radial symmetry. The common feature of the two systems is that there is only one fluid inlet. Measurements are reported for the mean size of various samples of real colloids, such as dextran macromolecules, emulsion paints, and milks, and a comparison is made with measurements using hydrodynamic chromatography (HDC), and photon correlation spectrometry (PCS).

### 1. INTRODUCTION

Despite recent advances in techniques such as photon correlation spectrometry (PCS) and gel permeation chromatography (GPC), the separation and characterization of large macromolecules and small colloidal particles still poses many practical problems and there is no generally accepted method. Work by Giddings (1) and others indicates that the various versions of field-flow fractionation (FFF) seem to offer many advantages, notably being well adapted to the colloidal size range (1 nm to 1  $\mu\text{m}$ ) and

giving a real physical separation of the species by size. Here we use a version of FFF, called flow field flow fractionation (F.FFF), which has the advantage of experimental simplicity by requiring only a single liquid flow and a filter membrane. A detailed theory of the hydrodynamics of the two systems presented here (asymmetrical channel with a plane membrane and a tubular channel with hollow fiber membrane) has been published elsewhere (2-4). This paper presents an experimental investigation with a wide range of type of colloids. Similar systems have also been investigated experimentally though with a less rigorous theoretical analysis which does not take into account nonuniform permeation along the length of the membrane. These include Wahlund et al. (5), who used the term F.FFF, Doshi et al. (6, 7), who called the technique polarization chromatography, Lee et al. (8), who used the term single phase chromatography, and, more recently, Jonsson et al. (9), who used a hollow fiber module similar to that used here. In general, these papers give experimental results for a more restricted range of colloids and with a less rigorous theoretical analysis which does not take into account nonuniform permeation along the length of the membrane.

## 2. OPERATING PRINCIPLE

As in any conventional chromatographic technique, analysis by F.FFF is based on the measurement of the transit time of a sample carried through a separating system by a constant flow of eluent. In this case the retention of the colloidal species depends on their size. However, as opposed to conventional liquid- or gas-phase chromatography which involve a stationary phase and a mobile phase, here we have only one phase which is the liquid eluent.

Two separating devices have been used here, both of very simple geometry. One is a thin (365  $\mu\text{m}$ ) rectangular channel of which one wall is a porous membrane, and the other is a narrow tubular porous channel formed by a hollow ultrafiltration fiber (diameter 230  $\mu\text{m}$ ). These are shown schematically in Fig. 1.

In both systems a single inlet flow is divided into two outlet components. One component passes through the channel as the carrier fluid, and the other passes through the membrane to form the polarized layer. In the experiments described here the total flow rate into the channel is controlled by a constant flow rate liquid chromatographic pump, and the flow rate through the membrane is controlled by aspiration with a constant flow rate peristaltic pump.

This flow system creates a transversal flow component (radial in the case of the hollow fiber) which brings about a distribution of the colloidal species

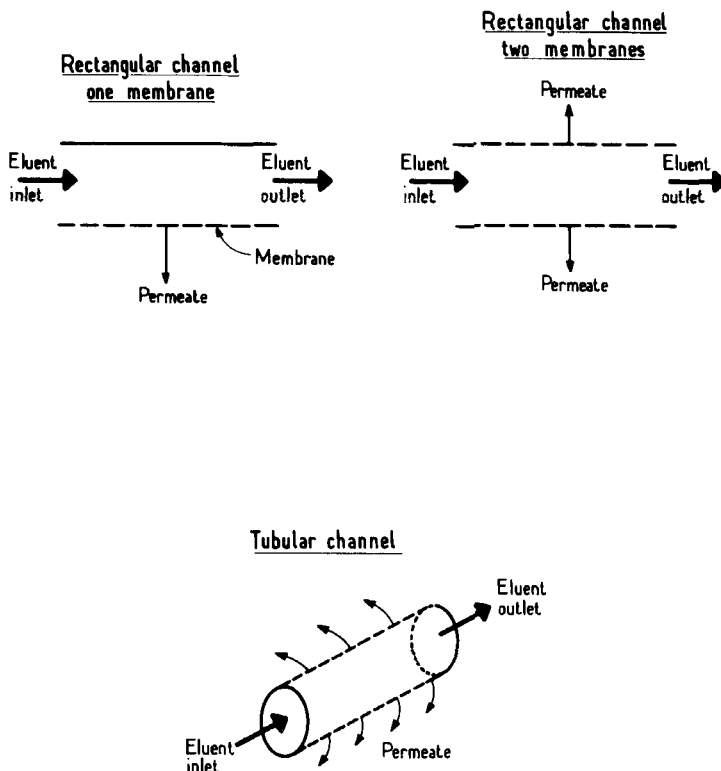


FIG. 1. Two types of FFFF module.

across the channel as shown schematically in Figs. 2 and 3. Since the colloids cannot pass through the membrane, a high colloid concentration is created at the membrane, which then tends to be redistributed across the channel by Brownian motion. After a certain time an equilibrium is attained between colloid transport to the membrane by convection and away from the membrane by diffusion, resulting in a quasi-exponential concentration profile which depends on the flow conditions and the diffusion coefficient of the colloids, and hence their size. The larger the particles, the lower their diffusion coefficient and the closer they remain to the filtering membrane. This same phenomenon, of the formation of concentrated layers at a membrane, is encountered in cross-flow filtration systems and, by analogy with electrolysis, is called concentration polarization.

The concentration gradients thus formed are moved through the channel by the velocity profile of the axial flow. The larger species located near

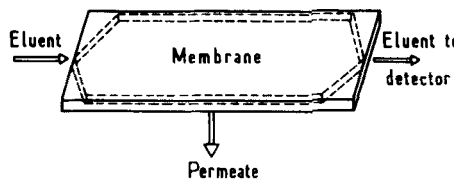
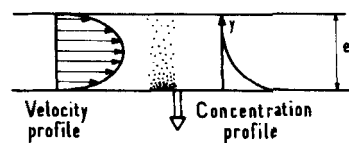


FIG. 2. Schematic diagram of a single membrane rectangular channel FFFF module.

the membrane are moved through the channel by the slow velocity component near the channel wall, and the smaller species, which tend to be toward the center of the channel, are moved along by the higher velocity component. The result is that the smaller species pass through the channel more rapidly than the larger species.

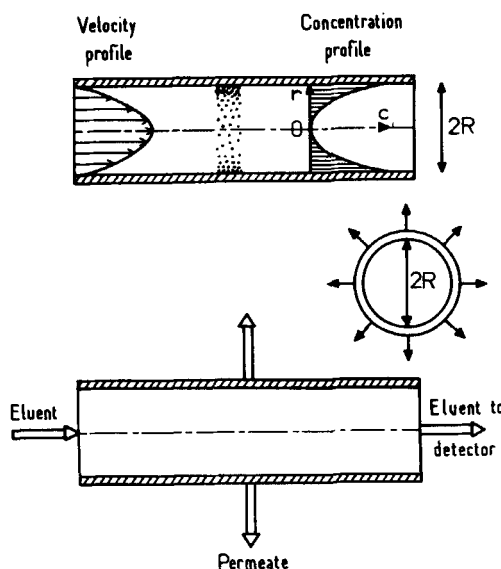


FIG. 3. Schematic diagram of a hollow fiber tubular channel FFFF module.

We have made a full theoretical analysis of the interplay between flow and diffusion for the separation of species by their size which has been presented elsewhere (2-4). Rigorous analytic solutions for the axial and tangential flow fields have been developed, and they show that in these systems, driven by internal pressure, the permeate flow through the membrane is greater at the inlet end than at the outlet end, and the variation is not linear along the length of the channel. Furthermore, in the case of an asymmetric rectangular channel, the velocity profile in the channel is not strictly parabolic, being slightly deformed by the transverse flow field. In conditions where the membranes are not too permeable and the channels not too long, these results reduce to the simplified flow fields used in other work (7, 8). Criteria have been established for determining the limits of applicability of the simplified solutions.

The transport behaviors of colloids in this flow field have been determined by obtaining an asymptotic solution to the convection-diffusion equation by using the method of Doshi et al. (7) in terms of the retention factor  $R_f$  and the Peclet number at the membrane  $Pe_w$ , defined as

$$R_f = \frac{\text{mean transit time of the carrier fluid}}{\text{mean transit time of the particles}} = \frac{t_m}{t_p} \quad (1)$$

$$Pe_w = V_w e / D \quad (2)$$

Here  $D$  is the diffusion coefficient (related to the particle diameter through the Stokes-Einstein equation),  $V_w$  is the mean permeation rate through the membrane (total flow rate through the membrane divided by the total membrane area), and  $e$  is the characteristic dimension of the channel (width of a rectangular channel or radius of a tubular channel). The analytic expressions relating particle size, flow rate, and retention time are given below for the two types of channel considered. For a rectangular channel with one porous wall:

$$R_f = -[1 - Pe_w/84 - 191Pe_w^2/46,200 + \dots] \quad \text{for } Pe_w < 8 \quad (3)$$

$$R_f = -6/Pe_w[1 - 2/Pe_w + 42/Pe_w^2 - 604/Pe_w^3 + \dots] \quad \text{for } Pe_w > 20 \quad (4)$$

For a tubular channel with radial symmetry:

$$R_f = -[1 + Pe_w/24 - Pe_w^2/1,440 + 101Pe_w^3/483,840 + \dots] \quad \text{for } Pe_w < 8 \quad (5)$$

$$R_f = -4/\text{Pe}_w [1 - 4/\text{Pe}_w + 72/\text{Pe}_w^2 - 1,485/\text{Pe}_w^3 + \dots]$$

for  $\text{Pe}_w > 20$  (6)

This shows that for a given system there is a single calibration curve  $1/R_f = f(\text{Pe}_w)$  which is linear for sufficiently high values of  $\text{Pe}_w$  and has a slope which depends on the geometry of the system (1/6 for a rectangular channel with one wall and 1/4 for a tubular channel). An example of the variation of  $1/R_f$  vs Peclet number at the permeable wall is given in Figs. 9 and 11. Measurement of the retention time of an unknown species and knowledge of the mean residence time of the carrier fluid and the mean permeation rate together with the calibration curve therefore allows us to determine the size of the unknown colloid. For further details, not necessary for explaining the results reported here, the reader should refer to the original publications (2-4).

### 3. DETAILS OF THE TWO TYPES OF MODULE

#### 3.1. Rectangular Channel F.FFF Module

Figure 4 gives an exploded view of the rectangular channel F.FFF module used in our experiments. The design is very similar to that used in cross-flow ultra- or microfiltration units as well as to those used by Giddings (1) for FFF. It is composed of two blocks of Plexiglas ( $4.5 \times 11 \times 70$  cm) held together by 28 nuts and bolts. Between these blocks are held in succession: a membrane support plate made of sintered stainless steel (pore size 8  $\mu\text{m}$ ), an ultrafiltration membrane (Iris 3038 polysulfone cut-off 10,000 MW made by Rhône Poulenc), and a spacer of Mylar rigid plastic 350  $\mu\text{m}$  thick in which the channel (length 60 cm, width 1 cm) is cut. Sealing between these is by O rings. The space under the membrane support plate is divided into five compartments each connected to a separate channel of a multtube peristaltic pump to ensure that flow through the membrane is equally distributed along its length. Liquid inlet and outlet are through orifices drilled in the upper Plexiglas block, and the ends of the channel are tapered to aid even fluid distribution.

#### 3.2. Tubular F.FFF Module

This module, shown in Fig. 5, comprises an ultrafiltration hollow fiber (type 110 polysulfone ultrafiltration fiber made by the team of P. Aptel, Université Paul Sabatier, Toulouse, France, with a rating of 10,000 molecular weight) held in a Plexiglas jacket. The jacket has an inside diameter of 1 cm and is about 2 m long with a screw tension system to hold the fiber

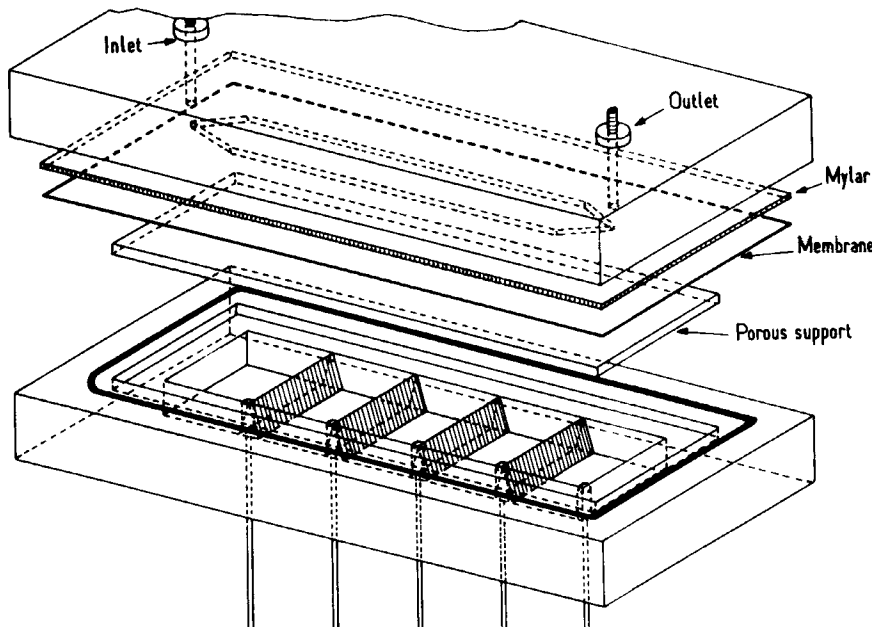


FIG. 4. Construction details of the rectangular channel FFFF module with a single flat membrane.

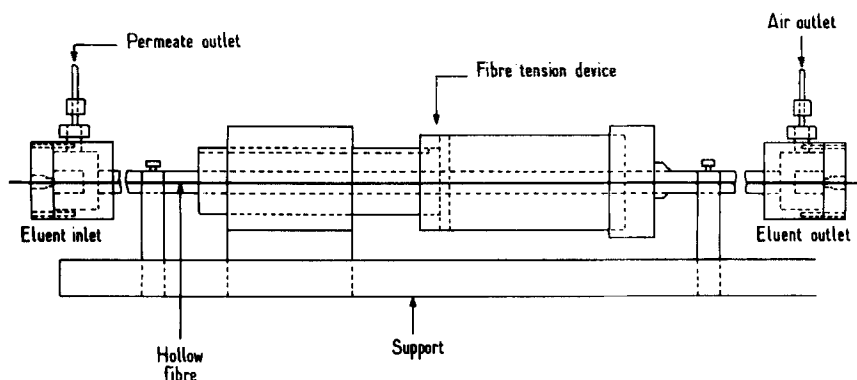


FIG. 5. Construction details of the tubular channel FFFF module with a hollow fiber.

straight in the center of the module and allow for variations in different fiber lengths. The permeate outlet is by a single point near the eluent inlet. The air outlet is used to aid the initial filling of the apparatus.

### 3.3. Experimental Apparatus

One or the other module is fitted in a conventional liquid chromatographic circuit as shown in Figs. 6 and 7. This comprises a constant flow liquid chromatographic pump (Gilson 302) with a pulse damper, an injection valve (Rheodyne 7125) with a 20- $\mu$ L loop, and either a UV detector set to 254 nm (Waters Lambda Max 481) or a differential refractometer (Waters R404). These are connected to a recorder and an integrator (Intersmat minigrator).

In the case of the rectangular channel module, the permeate flow is controlled by an Ismatec 5 channel peristaltic pump which ensures a uniform and fully controllable permeation rate along the length of the module, which allows experimentation on the influence of the permeation rate on the separation.

In the case of the tubular module, the permeation flow is pumped from the external jacket at a single point close to the input end. The theoretical analysis mentioned in Section 2.1 predicts that the permeate flow is not uniform along the length of the fiber, being greater at the inlet end than at the outlet end.

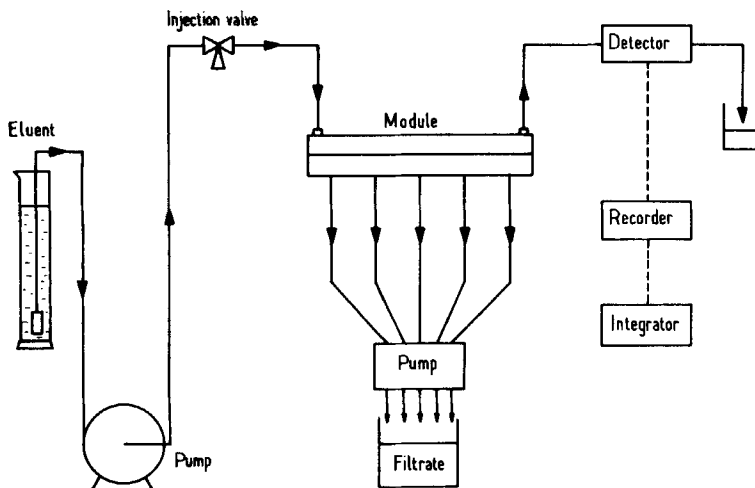


FIG. 6. Schematic diagram of the experimental set-up for the rectangular channel module.

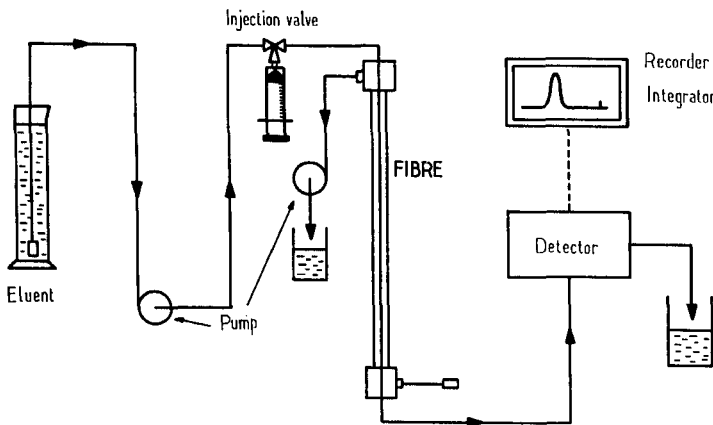


FIG. 7. Schematic diagram of the experimental set-up for the tubular channel module.

### 3.4. Experimental Conditions

The input flow rates into the modules were from 0.1 to 1 mL/min with the rectangular channel and 0.1 to 0.5 mL/min with the tubular channel. The average output flow rates were close to 0.02 mL/min, and practically the whole of the input flow passed through the membrane. The average permeation rate was determined from the flow rate through the membrane divided by the total membrane surface. The carrier fluid used in all experiments reported here was prepared with high resistivity deionized water (Milli-Q) with 0.13 g/L sodium azide ( $\text{NaN}_3$ ) as a bactericide and 0.75 g/L sodium dodecylsulfate (SDS) to give an ionic strength of 2.6 mM. The solutions were filtered through a 0.22- $\mu\text{m}$  Millipore membrane before use.

20  $\mu\text{L}$  samples of a 0.01% suspension were injected, and the resulting peaks were noted on the recorder and the integrator.

## 4. RESULTS

### 4.1. Calibration with Standard Particles

Calibration was made with standard latex particles ranging from 0.05 to 1  $\mu\text{m}$  in size. To extend the calibration below this range, we also used a sample of fluorescein isothiocyanate dextran of molecular weight 67,000 which has a size of 0.015  $\mu\text{m}$  as measured by a Malvern 4600 Photon Correlation Spectrophotometer.

#### 4.1.1. Results Obtained with the Rectangular Channel Module

Figure 8 gives an example of a chromatogram obtained with the rectangular channel for separate injections of samples of dextran with a molecular weight of 67,000 and latex particles of size 0.085, 0.091, and 0.145  $\mu\text{m}$ . The eluent was SDS 2.6 mM with an input flow rate of 0.2 mL/min and a permeate flow of 0.18 mL/min.

It can be seen that the chromatogram for the latex particles has two peaks for each sample. The first, with a sharp initial rise and a long tail, is always located at the same place whatever the size of the particles. This depends on the hydrodynamics in the system and corresponds to particles carried by the axial flow and unaffected by lateral migration or diffusion. The peak maximum is located at a residence time of  $2t_m/3$ , where  $t_m$  is the mean residence time in the system, as would be expected for pure convective flow in this rectangular channel.

The second peak, which is more spread out and relatively symmetrical, is located at longer times, the larger the size of the particle in the sample. This may be considered to be the peak predicted by the theoretical analysis corresponding to particles attaining a position near the membrane under the effects of convection and diffusion. Similar double peak responses have

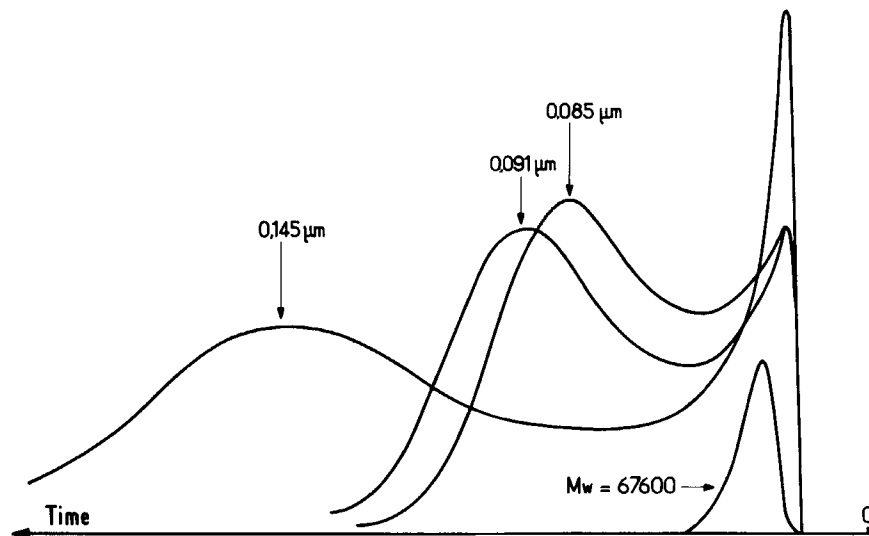


FIG. 8. Experimental results for samples of standard latex particles using the rectangular channel module. (Eluent solution SDS, 2.60 mM; inlet flow rate, 0.2 mL/min; flow rate through the membrane, 0.18 mL/min.)

been obtained by others for simple flow in tubes where the characteristic length was too short for Taylor dispersion analysis to apply; for example, Korenaga et al. (10).

Closer examination of these results reveals that the relative height of the two types of peak varies with the size of the particles (3). Using smaller and smaller particles reduces the height of the first peak and increases the height of the second peak. For very small, highly diffusive species, such as the dextran samples, the first peak is completely absent and we only observe the second peak. These effects may be interpreted as being due to larger particles having a lower diffusion coefficient and not having sufficient time to attain an equilibrium concentration profile at the membrane. The transport mechanism in the channel involves axial and transversal convection, and diffusion. The presence of two peaks in the response indicates that some of the particles are transported through the channel by axial convection before the effects of transverse convection and diffusion have had time to act.

Other workers (5, 9) have overcome this problem by using a "relaxation" technique where axial flow is stopped to allow time for the concentrations profiles to become established before elution. This was not used in our experiments because stopping and restarting flow leads to pressure transients which perturb the experiments. Nevertheless, the differences shown in the residence times of the symmetrical peaks indicate that nonequilibrium FFFF can be used as an analysis method. Furthermore, the experimental procedure is simpler by being nondiscontinuous, which would be an advantage if used with automatic sample injection. We have therefore carried out experiments to study the influence of permeation rate on the  $R_f$  values corresponding to the second peak to determine whether it is a function of  $Pe_w$  as predicted by the theory.

Figure 9 gives a calibration curve of  $1/R_f$  vs  $Pe_w$  for the flat channel for different samples of standard particle and different permeation rates. It can be seen that there is a linear relation between  $Pe_w$  values of 20 and 80. As expected from the theoretical analysis,  $1/R_f$  is always greater than 1, and tends to 1 when  $Pe_w$  tends to zero. However, the slope of the experimental curve is 1/8.5 as compared to the predicted slope of 1/6. As mentioned above, the fact that the system has not fully attained the expected equilibrium may explain this difference.

#### 4.1.2. Results Obtained with the Tubular Module

Figure 10 shows the chromatograms obtained with the tubular module by using standard latex particles in the size range 0.085 to 0.794  $\mu\text{m}$  with 2.60 mM SDS as the carrier fluid. As with the rectangular module, each

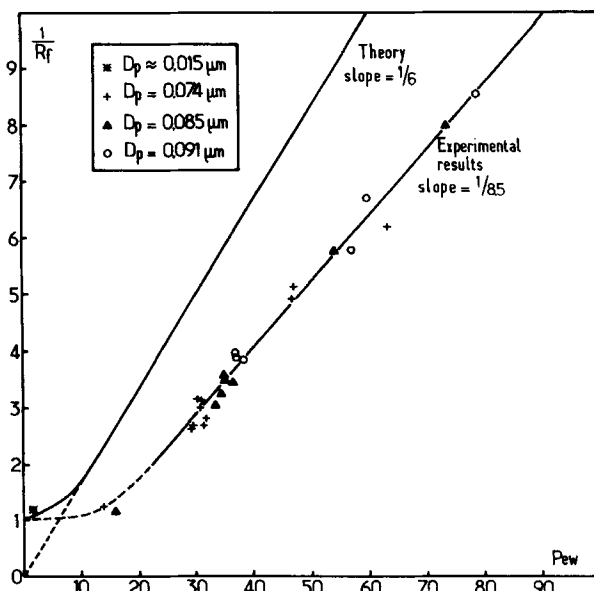


FIG. 9. Calibration curve for the rectangular channel module,  $1/R_f$  versus  $Pe_w$ .

sample injection in the tubular module also produces two peaks. As before, the first of these has a sharp front followed by a long tail, but here it is located at  $t_m/2$  because the maximum axial flow rate in laminar flow in a tube is twice the mean flow rate. The second peak is more symmetrical and has a higher residence time, the larger the particles concerned. The same analysis of the interplay between diffusion and convection may be made and, as before, the results show the variation in retention which is obtained for different sizes of particle.

The tubular module allows a wider range of operating flow conditions than does the rectangular cell, and an extensive series of experiments was performed at different permeate flows. One example for a range of different particles with a fixed wall permeation flow rate are shown in Fig. 11 as curves of  $1/R_f$  versus  $Pe_w$ . Figure 14 gives other results for a single size of particle, here dextran T500, where the wall flow rate has been varied.

Over the range of operating conditions allowed by the tubular module, it was found that, in general, the calibration curves have a convex shape and can only be considered to be linear for Peclet numbers below 100. In addition, over the month or so that a given fiber was in use, we found a progressive drift in the calibration curves. Theoretical analysis indicates

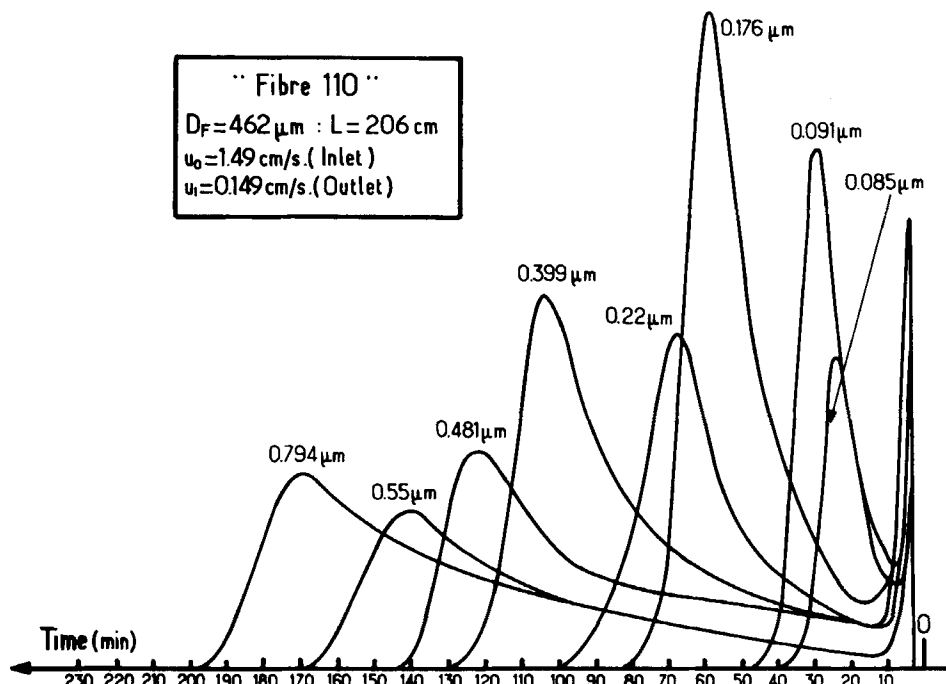


FIG. 10. Experimental results using the tubular channel module for separate injections of standard latex particles.

the importance of the dimensions of the channel and the membrane permeability on the uniformity of permeate flow along the length of the membrane. Accordingly, a long tubular channel having a high permeability is thus expected to have a greater permeate flow near the channel inlet than at the channel outlet, which may be considered to lead to this sort of nonlinearity. Furthermore, the dimensional changes due to pressure and changes in membrane permeability due to progressive clogging may explain the variability with use. As for the rectangular channel, the results do not agree with the theoretical prediction of a single linear calibration curve having a slope of 1/4 ( $Pe_w > 20$ ).

Figure 12 shows the effects of permeation flow rate on the separation of a mixture of standard latex particles of sizes 0.091 and 0.176  $\mu\text{m}$  in suspension in a 2.60 mM SDS carrier fluid. It can be seen that higher permeation rates increase resolution at the expense of longer analysis times. Figure 13 gives an example of the separation of a three component mixture of standard latex particles of sizes 0.085, 0.22, and 0.55  $\mu\text{m}$ .

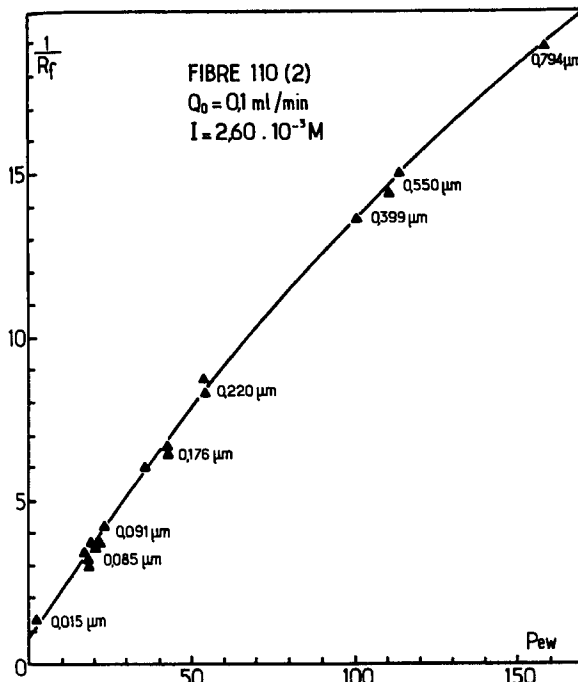


FIG. 11. A calibration curve for the tubular channel module,  $1/R_f$  versus  $Pe_w$ . The figures refer to the diameters of standard latex particles.

#### 4.2. Measurements with Various Types of Colloid

In Table 1 we present the results obtained using FFFF for determining the size in various colloidal suspensions. The particle sizes obtained are compared with measurements made by two other techniques: hydrodynamic chromatography and photon correlation spectrometry, which are reported elsewhere (11). Results obtained with dextran macromolecules are also given and compared with a mean particle size calculated from their molecular weight and intrinsic viscosity.

The method used is to inject a sample of the unknown colloid in suspension in 2.6 mM SDS and determine the  $R_f$  value of the output peak. A Peclet number  $Pe_w$  is then read off the calibration curve established with the standard latex particles. Knowing the permeation rate then allows determination of a diffusion coefficient, from which an equivalent particle diameter can be calculated using the Stokes-Einstein equation. Generally several successive injections of the same sample are made at different permeate flow rates. Figure 14 shows such results for the case of dextran

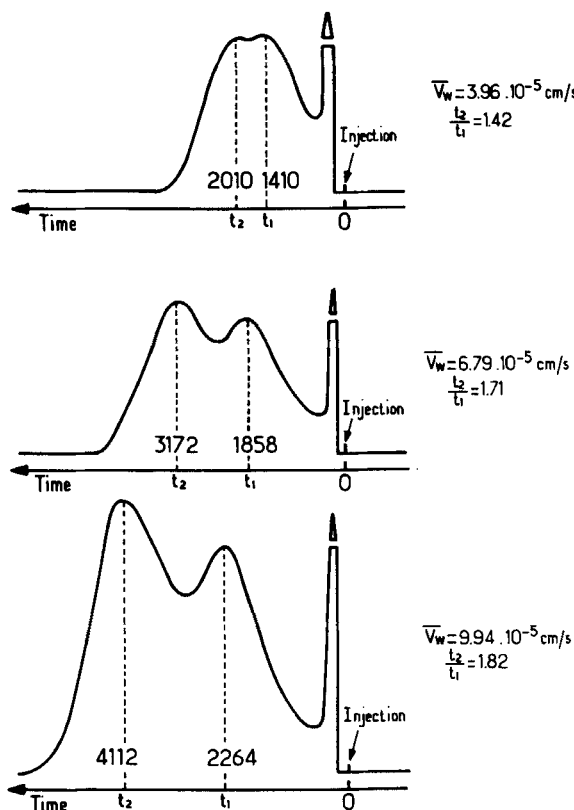


FIG. 12. Effect of mean permeation rate  $V_w$  in the tubular channel module on the separation of a mixture of two sizes of standard latex particles: 0.091 and 0.176  $\mu\text{m}$ .

T500 which are used to give an average equivalent diameter. The fact that all the points lie close to the same curve indicates that the technique gives very reproducible results.

Table 1 gives the mean particle size obtained for a range of colloids together with comparative values determined by other techniques or by calculation from known properties. It can be seen that there is a certain degree of agreement between the equivalent diameters obtained by FFFF and by hydrodynamic chromatography (HDC) and PCS as with the size of polymer molecules determined from their molecular weights.

The results obtained with the fractionated *Dextran* samples (Pharmacia Dextran T fractions), assuming the macromolecules to be spheres and that the calibration curve is linear for  $\text{Pe}_w$  less than 100, gives equivalent

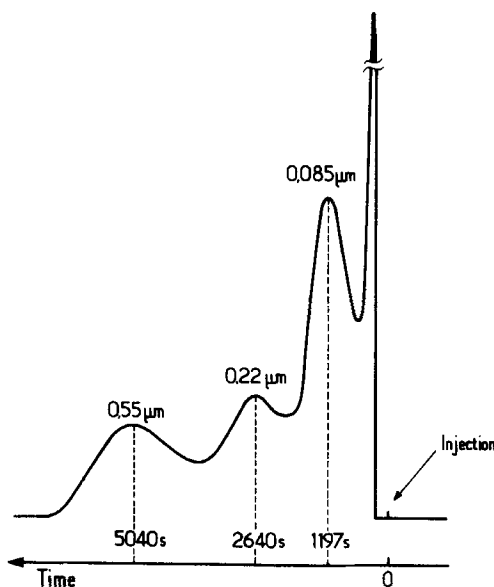


FIG. 13. Separation of a mixture of three standard latex particles in the tubular channel module. (Eluent SDS, 2.6 mM; inlet flow rate, 0.1 mL/min; flow rate through the membrane, 0.075 mL/min.)

TABLE 1  
Results of Analysis of Various Colloidal Suspensions by F.FFF, HDC, and Photon Correlation Spectrometry (PCS)

Sample	Type	Rectangular channel equivalent diameter (nm)	Tubular channel equivalent diameter (nm)	HDC equivalent diameter (nm)	PCS equivalent diameter (nm)	Calculated equivalent diameter (nm)
Dextrans	T10	30	4		5	
	T40		12		10	
	T70		14		13	
	T500		33	45	33	
	T2000		42	85	56	
Xylophene			20	100	130	
Stabisol		18	15	40	33	
Ludox	TM		23	100	43	
	HS 40		19		20	
UHT milk	Full cream		500	490	440	
	1/2 cream		400		350	
Mat paint	Theodore	400	240		205	
	AVI 3000		400	600	420	

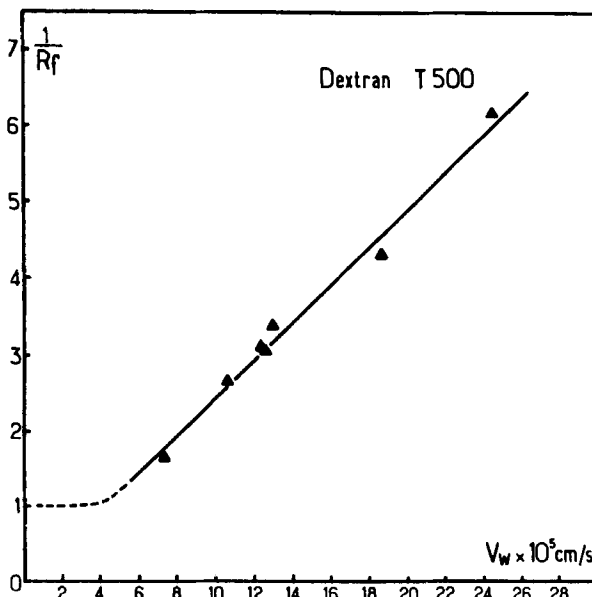


FIG. 14. Variation of  $1/R_f$  with mean permeation rate  $V_w$  in the rectangular channel for Pharmacia Dextran T500 (nominal molecular weight 500,000).

diameters which increase with increasing molecular weight and which are close to the values calculated using the Mark-Houwink equation and molecular parameters given by the supplier.

The equivalent diameters obtained for the samples of *Xylophene*, *Stabisol*, and *Ludox* are smaller than those measured by HDC and PCS. (*Xylophene* is an industrial phenolic emulsion provided by Rhone Poulenc, *Stabisol* is a silica sol used for calibrating industrial turbidimeters provided by Tepral, and *Ludox* TM and HS 40 are colloidal silica dispersions purchased from E. I. du Pont de Nemours.) These differences may be explained by the fact that the sizes involved here are below the range of calibration of HDC and require extrapolation of the calibration curves. The curvature of these is rather pronounced near the origin and extrapolation is uncertain. In PCS, agglomeration and contamination by larger particles in suspension cannot be excluded.

The analyses involving *UHT milk*, probably relating to caseine micelles, show good agreement between the three techniques F.FFF, HDC, and PCS.

The same conclusion is obtained for the experiments on *Acrylic emulsion paint* (both samples are commercial household products). However, the results obtained by HDC are rather different. This can be attributed

to aging of the sample because more than a year separated the HDC experiments from those of PCS and F.FFF.

## 5. CONCLUSIONS

These results demonstrate that, even when an equilibrium regime is not attained, F.FFF does offer a means of characterizing colloidal suspensions, macromolecules, and emulsions. Reproducible values of equivalent diameter are obtained despite the variability involved in working with these inherently unstable products. The equipment is relatively simple with the important advantage of treating samples in their natural suspension medium and not subjecting them to physical or chemical effects which could denature them. Furthermore, F.FFF offers only a very small solid surface to the species under investigation and is thus less subject to adsorption or reaction interactions, and the very simple, uniform geometry of the channels means that the danger of degradation by shear forces is much reduced, which may be important when characterizing emulsions. Another advantage is that separation can be controlled by the permeation rate, and hence the retention of species can be varied by simple adjustment of the relative flow rates through the channel and through the membrane. This makes the system more flexible than HDC and GPC, and it allows a wide size range to be examined in the same apparatus. The lower limit of measurement is that of the exclusion limit of the membrane, the upper limit depending on the time allowable for diffusion to take place and, in any case, around 1  $\mu\text{m}$ . Diffusion becomes much less important than other transport phenomena above this size.

## NOMENCLATURE

$D$	diffusion coefficient ( $\text{m}^2/\text{s}$ )
$D_f$	inside diameter of fiber (m)
$D_p$	particle diameter (m)
$D_{p1}, D_{p2}$	two values of particle diameter (m)
$e$	thickness of rectangular channel (m)
$L$	channel length (m)
$\text{Pe}_w$	Peclet number at wall (defined in Eq. 2) (—)
$Q_0$	flow rate into channel ( $\text{m}^3/\text{s}$ )
$Q_1$	flow rate out of channel ( $\text{m}^3/\text{s}$ )
$Q_2$	permeate flow rate ( $\text{m}^3/\text{s}$ )
$R$	fiber radius (m)
$R_f$	retention factor (defined in Eq. 1) (—)
$t$	time (s)
$t_1, t_2$	two values of time (s)

$t_m$	mean residence time of fluid (s)
$t_p$	mean residence time of particles (s)
$V_w$	mean permeation velocity over the whole of the membrane (m/s)
$V_{w1}, V_{w2}$	two values of mean permeation velocity (m/s)
$w$	width of the rectangular channel (m)

## REFERENCES

1. J. C. Giddings, M. N. Myers, K. T. Caldwell, and S. R. Fisher, "Analysis of Biological Macromolecules and Particles by Field-Flow Fractionation," *Methods Biochem. Anal.*, **26**, 79-136 (1980).
2. J. Granger, "Ecoulement tangentiel de suspensions colloïdales au voisinage d'une membrane filtrante. Chromatographie de polarisation," Doctorate Thesis, INPL Nancy, France, November 1986.
3. J. Granger, J. A. Dodds, D. Leclerc, and N. Midoux, "Flow and Diffusion of Particles in a Channel with One Porous Wall: Polarization Chromatography," *Chem. Eng. Sci.*, **41**, 3119-3128 (1986).
4. J. Granger, J. Dodds, and N. Midoux, "Laminar Flow in Channels with Porous Walls," *Chem. Eng. J.*, **42**, 193-204 (1989).
5. K. G. Wahlund and J. C. Giddings, "Properties of an Asymmetric Flow Field Flow Fractionation Channel Having One Permeable Wall," *Anal. Chem.*, **59**, 1332-1339 (1987).
6. M. R. Doshi, W. N. Gill, and R. S. Subrahmanian, "Unsteady Reverse Osmosis or Ultrafiltration in a Tube," *Chem. Eng. Sci.*, **30**, 1467-1476 (1975).
7. M. R. Doshi and W. N. Gill, "Pressure Field-Flow Fractionation or Polarization Chromatography," *Ibid.*, **34**, 725-731 (1979).
8. H. L. Lee, J. G. Reis, J. Dohner, and E. N. Lightfoot, "Single Phase Chromatography: Solute Retardation by Ultrafiltration and Electrophoresis," *AIChE J.*, **20**, 776-784 (1974).
9. J. A. Jonsson and A. Carlshaf, "Flow Field Fractionation in Hollow Cylindrical Fibers," *Anal. Chem.*, **61**, 11-18 (1989).
10. T. Korenaga, F. Shen, and T. Takahashi, "An Experimental Study of the Dispersion in Laminar Tube Flow," *AIChE J.*, **35**, 1395-1398 (1989).
11. M. Leitzlement, J. Dodds, and D. Leclerc, "Measurement of the Particle Size of Sub-micron Mineral Particles, Emulsions and Biological Material by Hydrodynamic Chromatography and Photon Correlation Spectroscopy," in *Particle Size Analysis 1985* (P. J. Lloyd, ed.), Wiley, New York, 1987.

Received by editor July 15, 1991

Revised March 11, 1992